Exp Fluids
DOI 10.1007/s00348-010-0954-5

RESEARCH ARTICLE

Diffusive mixing through velocity profile variation in microchannels

Ehsan Yakhshi-Tafti · Hyoung J. Cho · Ranganathan Kumar

Received: 8 December 2009 / Revised: 16 May 2010 / Accepted: 3 August 2010

Abstract Rapid mixing does not readily occur at low Reynolds number flows encountered in microdevices; however, it can be enhanced by passive diffusive mixing schemes. This study of micromixing of two miscible fluids is based on the principle that (1) increased velocity at the interface of co-flowing fluids results in increased diffusive mass flux across their interface, and (2) diffusion interfaces between two liquids progress transversely as the flow proceeds downstream. A passive micromixer is proposed that takes advantage of the peak velocity variation, inducing diffusive mixing. The effect of flow variation on the enhancement of diffusive mixing is investigated analytically and experimentally. Variation of the flow profile is confirmed using micro-Particle Image Velocimetry (μPIV) and mixing is evaluated by color variations resulting from the mixing of pH indicator and basic solutions. Velocity profile variations obtained from μPIV show a shift in peak velocities. The mixing efficiency of the Σ-micromixer is expected to be higher than that for a T-junction channel and can be as high as 80%. The mixing efficiency decreases with Reynolds number and increases with downstream length, exhibiting a power law.

Abbreviations

Re	$\rho \bar{U} d_H / \mu$
Pe	$\bar{U} d_H / D$
μ	Dynamic viscosity
ρ	Density
D	Diffusion coefficient
v_z ($v_{\max}$)	Velocity (maximum)
δ	Film thickness
c	Concentration
N	Mass flux
τ	Residence time
H, h, a, b, R, λ	Design parameters
σ	Standard deviation
I	Grayscale color intensity
L	Mixer length
M	Mixing percentage
$\bar{U}$	Average velocity
$u^* = U/\bar{U}$	Normalized velocity
w^*	Normalized width

E. Yakhshi-Tafti · H. J. Cho · R. Kumar (✉)
Department of Mechanical, Materials & Aerospace Engineering, University of Central Florida, Orlando, FL 32816, USA
e-mail: Rnkumar@mail.ucf.edu

H. J. Cho
School of Advanced Materials Science & Engineering, Sungkyunkwan University, Suwon, Korea

1 Introduction

Microfluidic devices are mainly designed for chemical and biological applications where rapid and efficient mixing is essential. Mixing is of considerable importance in lab-on-a-chip (LOC) bio-analysis systems since a majority of the applications often involves reactions that require quick and efficient mixing of reagents (Liu et al. 2000). Nevertheless, mixing is greatly limited in microscale laminar flow devices. In highly laminar flows, introduction of chaos and turbulence cannot be easily achieved or may not be practical under design constraints; therefore, rapid mixing is not readily possible in microfluidic devices. Transport processes at microscales are diffusion-based and are not due to inertial effects. This limitation is the motivation for an in-depth study of diffusive mixing in microchannels.

Published online: 18 August 2010

Mixing can be enhanced either by introducing external sources of stimulation such as acoustic (Liu et al. 2002), thermal (Tsai and Lin 2002), electrokinetic (Oddy et al. 2001) and pressure disturbances (Deshmukh et al. 2001) that cause stirring effects in order to enhance mixing of reagents. On the other hand, passive mixers implement geometrical features of channels or turbulent/chaotic flow to improve mixing (Hardt et al. 2005; Lee et al. 2006; Liu et al. 2000, 2009; Nichols et al. 2005; Schonfeld et al. 2004). Due to cost and fabrication issues, two-dimensional (planar) passive mixers are preferred (Hong et al. 2004; Melin et al. 2004; Tofteberg et al. 2009) over complicated three-dimensional microstructures.

In this study, experiments have been conducted to evaluate the effect of the velocity profile on diffusion by comparing mixing in a straight microchannel (T-mixer) and a serpentine-like microchannel (Σ-mixer) with special sidewalls that alter the laminar velocity profile. These experiments also validate the theoretical groundwork that is established to gain an understanding of the underlying flow physics and identify the parameters that have an effect on diffusive mixing in laminar co-flowing liquids. First, an analytical framework for diffusion of species into a flowing film is provided to show how velocity at diffusion interfaces affects diffusive mass flux (mixing). Based on the theoretical findings, a Σ-shaped microchannel with periodically varying sidewalls is considered which can passively alter the laminar flow field. The diffusive mixing is studied experimentally by correlating color changes resulting from the mixing of a pH indicator solution and a base solution. Mixing efficiencies in the straight microchannel and the Σ-micromixer are compared. Finally, the velocity profiles are obtained in different cross sections of the Σ-micromixer using micro-Particle Image Velocimetry (μPIV) results to confirm the periodic and passive flow variation.

2 Experimental procedure

2.1 Preliminary analysis for micromixer design

Flow in microdevices is usually characterized by low Reynolds number and high Peclet number values (Nguyen and Wu 2005). In the current experiments, Reynolds number ranges from 0.1 to 4.5 and Pe ~ 1,000. Therefore, the dominating process in this micromixing is molecular diffusion. The diffusive mass flux across an interface of miscible media is proportional to the interfacial area and concentration gradient between the two. Furthermore, diffusion of species in co-flowing fluids occurs much slower in the transverse direction than in the streamwise direction of the flow. For non-flowing conditions, increasing the surface area and concentration gradient across an interface will increase diffusive flux of species for a given binary diffusion coefficient; for co-flowing fluids, however, there are other factors affecting the process of mixing.

In order to explain the micromixing strategy used in this study, a simplified model of the problem is considered in Fig. 1. A film of liquid (species *B*) is flowing with a given parabolic velocity profile, into which species *A* diffuses. It is assumed that diffusion of species would not alter the hydrodynamics of the laminar flow, and that the diffusion takes place slow enough that the diffused species would not penetrate very far into the liquid (Bird et al. 2007). The velocity profile considered could be of a general form:

$$v_z = v_{\text{int}}\left[1 - \left(x/\delta\right)^2\right] \tag{1}$$

where $x = 0$ is at the interface, v_z, v_{int}, δ are velocity, velocity at the interface and film thickness, respectively. Considering the fact that mass transfer is predominantly diffusion-based in x-direction and convection-based in z-direction, the governing transport equation for concentration distribution of species A, c_A is given as follows with $D_{A,B}$ as the binary diffusion constant:

$$v_z \frac{\partial c_A}{\partial z} = D_{A,B}\frac{\partial^2 c_A}{\partial x^2} \tag{2}$$

Substitution of Eq. 2 in Eq. 3 gives

$$v_{\text{int}}\left[1 - \left(x/\delta\right)^2\right] = D_{A,B}\frac{\partial^2 c_A}{\partial x^2} \tag{3}$$

Considering the large Pe number (ratio of streamwise advection to transverse diffusion of species ~1,000) species *A* does not penetrate a long distance compared to the thickness of the liquid film; hence, the variations of the velocity from the interface into depth and towards the wall (the parabolic profile) can be neglected and based on this approximation, the problem can be reduced to a problem of diffusion of A into a liquid film moving with the velocity v_{int}. The simplified governing equation becomes:

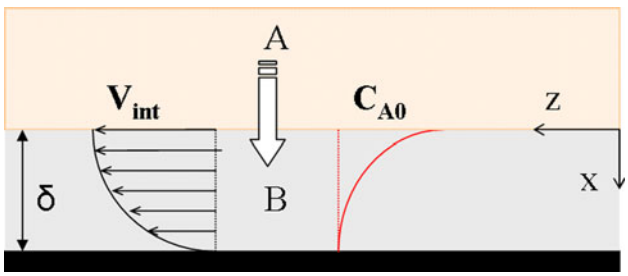

Fig. 1 Diffusion of species A into liquid film B; C_{A0} is the solubility limit of A into liquid B

$$v_{\text{int}}\frac{\partial c_{\text{A}}}{\partial z} = D_{\text{A,B}}\frac{\partial^2 c_{\text{A}}}{\partial x^2} \tag{4}$$

with the following simplified boundary conditions:

$$z = 0: c_{\text{A}} = 0;\ x = 0: c_{\text{A}} = c_{\text{A0}},\ \text{and}\ x = \delta: \partial c/\partial x = 0$$

By using similarity variables, the solution has the following form:

$$\frac{c_{\text{A}}}{c_{\text{A0}}} = 1 - \frac{2}{\sqrt{\pi}}\int_0^{\frac{x}{\sqrt{4D_{\text{A,B}}z/v_{\text{int}}}}} \exp(-\xi^2)d\xi = \text{erfc}\left(\frac{x}{\sqrt{4D_{\text{A,B}}z/v_{\text{int}}}}\right) \tag{5}$$

Knowing the concentration gradients, the local mass flux at the interface is found to be

$$N_{\text{A,interface}} = -D_{\text{A,B}}\frac{\partial c_{\text{A}}}{\partial x}_{@x=0} = c_{\text{A0}}\sqrt{\frac{D_{\text{A,B}}v_{\text{int}}}{\pi z}} \tag{6}$$

Equation (6) shows that if the mass flux—diffusion of species—across the interface is to be increased, then v_{int} has to be increased. This concept is important to mixing enhancement.

The other key element comes from the fact that, as the two fluids mix, the diffusion interfaces would shift away from the centerline coinciding with the slow moving layers as the flow moves downstream of the channel. The position of the diffusion interface of each of the species would progress from the centerline in the x-direction in both directions as follows:

$$X'(z) = \left(2D_{\text{A,B}}\tau\right)^{1/2} = \left(2D_{\text{A,B}}\cdot\frac{z}{U_{\text{ave}}}\right)^{1/2} \tag{7}$$

where X', τ and U_{ave} are displacement of interface from centerline, residence time and average fluid velocity, respectively. Thus, Eqs. (6) and (7) establish two key points: (1) diffusive mass flux across fluid layers with higher interfacial velocity is expected to be higher and (2) diffusion interfaces progress in the transverse direction (x) downstream of the channel. Diffusive mixing is limited in a straight channel (T-mixer) because the unchanging flow profile has a maximum fixed at the centerline and when diffusion interfaces move off the center they coincide with slow moving layers of fluid; due to key point (1) diffusive flux rapidly drops slowing down the overall mixing (Fig. 2a).

Since the interfaces migrate in the case of coflowing liquids, a strategy for enhancing diffusive mixing between them is to alter the velocity profile such that its maximum gets shifted or rather swept across the transverse direction; hence, repeatedly coinciding with the transversely progressing diffusion interfaces throughout the residence time of fluids in the mixing channel (Fig. 2b)

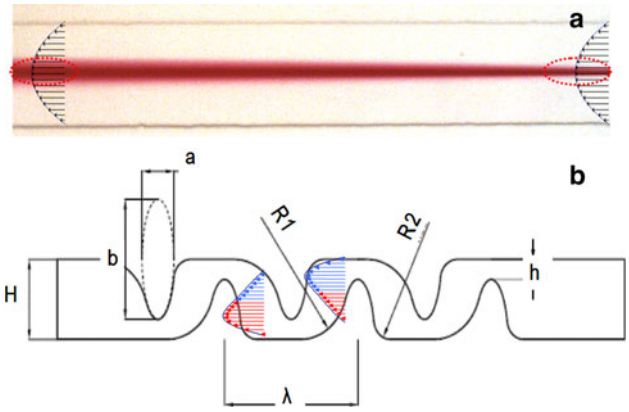

Fig. 2 **a** Maximum of the flow profile is always on the center in a T-mixer. **b** By using appropriate sidewalls, the laminar flow can be passively altered such that the maximum periodically sweeps the transverse direction coinciding with the transversely progressing diffusion fronts—higher interfacial velocity leads to better flux and better diffusive mixing

Based on the above analysis, a Σ-shaped micromixer is designed (Fig. 2b) where the shape of the sidewalls is important as it causes the flow profile to change in such a way that the maximum of the profile is not fixed at the center at all times and gets shifted periodically across the transverse direction passively. Due to the repeating patterns, the shift in maximum velocity would occur periodically and the progressing diffusion fronts and the maximum velocity layers of flow coincide repeatedly during the residence time of the fluid inside the mixing channel. This is in contrast with the conventional T-mixer in which the flow retains a parabolic profile downstream and the maximum velocity occurs only at the centerline. Detailed study relating the parabolic velocity profile on diffusion and the near wall effects is available (Ismagilov et al. 2000; Kamholz and Yager 2001) where the so-called *Butterfly effect* was detected in binary diffusion in microchannels. It was termed the *butterfly* since the width of the reaction–diffusion zone is not uniform across the depth of the channel. It is thinnest at the core of the flow and gets wider at the interfaces adjacent to the walls of the channel. The sidewall profiles of Σ-micromixer are generated by alternate circular/ellipsoidal shapes as shown in Fig. 2b. The upper and lower wall profiles repeat periodically with a phase lag causing nonsymmetric channel width variation with respect to the centerline. The parameters a and b define the ellipsoid used to generate the slopes with which sidewalls contract or expand; λ is the periodic length of the repeating sidewall profiles; H is predefined as channel width and h is the throat width ($H = 200$ μm, $h = 50$ μm, $a = 100$ μm, $b = 300$ μm, $R1 = 140$ μm, $R2 = 50$ μm, $\lambda = 400$ μm and with channel depth of 100 μm). These parameters make the sidewalls expand or

contract asymmetrically. Sharp corners are removed by making the walls smooth to ensure that no dead volumes are created in the device. Alternating acceleration and deceleration of the liquid layers relative to each other leads to a better mixing without the use of complex three-dimensional features and obstructions in the flow that could create stagnation or recirculation of the fluid in trap zones.

2.2 Micromixer fabrication

The Σ-micromixer has an in-plane structure which makes the fabrication and integration easier. It will be shown in this paper that passive mixing can be achieved efficiently with this design compared to complex three-dimensional geometries (Jen et al. 2003; Schonfeld et al. 2004; Stroock et al. 2002). Considering the applications of passive micromixers, ranging from single-use disposable assay chips to integrated microfluidic platforms for combinatorial chemistry and diagnostic devices used in pharmaceutical research, emphasis has been placed on having the simplest, yet effective structure.

Figure 3 shows the general fabrication procedure and the scanning electron microscopy (SEM) images of the fabricated devices (~100 μm deep, 200 μm wide at the largest width and 20 mm of mixer length). A typical procedure for fabricating a microchannel is soft lithography. A layer photoresist (SU8 Microchem®, MA) is spin coated on a polished substrate; the thickness of the coating, based on the spinning speed, would determine the height of the microchannels (15 s @ 500 rpm followed by 45 s @ 1,000 rpm). The *soft-bake* process consists of two stages (10 min @ 70°C followed by 30 min @ 105°C on a hotplate). SU-8 is a high-contrast, epoxy-based negative photoresist used for micromachining and other microelectronic and microfluidic applications, where thick, chemically and thermally stable features are desired. The next step is patterning via photolithography. SU-8 is optimized for near UV (350–400 nm) exposure (EVG 620 Mask Aligner, NY). The optimal exposure dose depends on film thickness (thicker films require higher dosage) and process parameters (total dosage for targeted thickness is within 350–400 mJ/cm^2). The UV light exposed and subsequently thermally cross-linked portions of the film are rendered insoluble to liquid developers. SU-8 is used to create high aspect ratio structures with near vertical walls in very thick films due to its optical properties. *Post exposure bake* is done directly after exposure in two steps (3 min @ 75°C followed by 10 min @ 105°C). After cooling, the SU-8 developer (Microchem®, MA) is used for developing the patterns. The fabricated SU-8 mold will be used to replicate patterns in the elastomer resin. Patterns can be replicated as many times, depending on the quality of the mold. Sylgard 184 Silicone® (Dow Corning, MI) is used for fabricating the microchannels. The elastomer is mixed with the curing agent and poured on the mold and allowed to cure eventually taking the shape of the patterned microcanals. The layer consisting of transferred patterns is bonded to another blank layer of PDMS or glass slide to create a closed fluidic channel by surface treatment (Corona treatment) to form closed microchannels. Inlet and outlet ports are punched in the blank layers prior to bonding.

2.3 Mass diffusion experiment using image processing

In order to observe the efficiency of the proposed micromixer and compare the effect of flow variation over

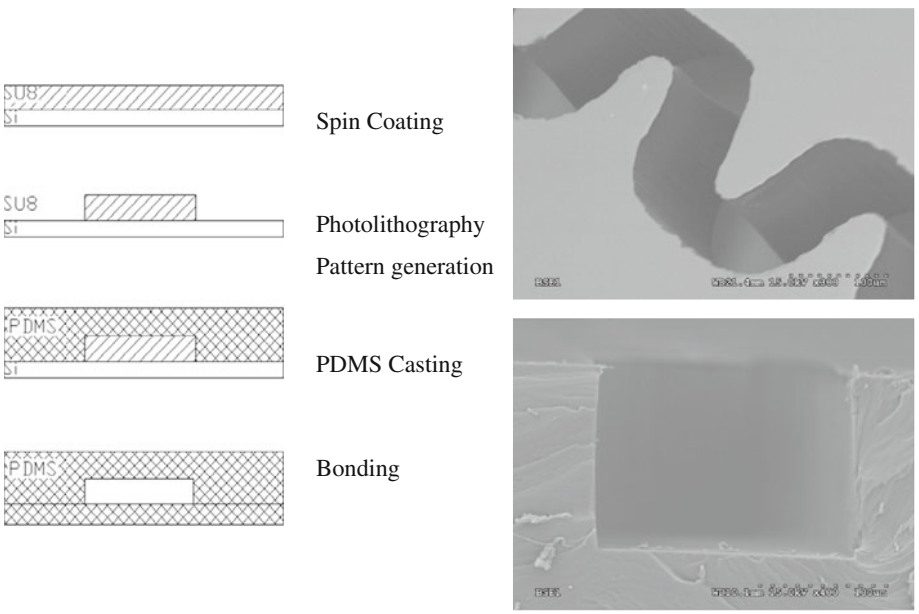

Fig. 3 (*Left*) General procedure for making microchannel using the SU8 resist and PDMS replication; (*right*) Scanning Electron Microscopy (SEM) oblique view of the micromixer channel (*top*) and the rectangular cross section (*bottom*)

the non-varying velocity profile in a T-mixer, a technique of chemical mixing/reaction to determine the extent of mixing has been adopted. An experiment was setup where two streams, a base solution (sodium hydroxide, pH = 12.5) and a pH indicator solution (phenolphthalein) were pumped into the mixer. Upon mixing, the transparent solutions turn into pink/purple color. Phenolphthalein solution (phenolphthalein 1%, isopropyl alcohol 60%, water balance) and 0.4 N sodium hydroxide solution (1.6% sodium hydroxide in a similar solution to above and pH = 12.5) were used. When mixed, a pink/purple region is formed which expands transversely, with two interfaces moving away from the centerline as the solutions further mix downstream. The intensity of the image can then be recorded and evaluated as explained in the Sect. 4; mixing is quantified by determining the standard deviation of color intensity from ideal mixing. Correlation has been provided between color intensity and complete and ideal mixing of reactants. Ideal mixing happens when all pixels across the width attain the darkest gray shade and the deviation among gray indices is zero.

2.4 Micro-particle image velocimetry

Micro-Particle Image Velocimetry (μPIV) is now a common technique to determine velocity fields in microchannels. This technique is used here to validate the periodic variation of the laminar flow profile expected from the sidewalls of Σ-micromixer. The μPIV (TSI Inc, MN) system (Fig. 4) used consists of an Nd:Yag laser source that generates green light at a wavelength of 532 nm. Nikon (TE2000-S) inverted microscope is used for magnifying the flow field compatible with the epi-fluorescent technique. Polystyrene fluorescent-dyed micro-spheres were used as the tracer particle with the following properties: 1 μm average diameter, 540 nm excitation/560 nm re-emission wavelength, 10^{10} beads/mL (FluoroSpheres, Invitrogen CA). A CCD camera was used to capture PIV images, capable of acquiring image-pairs at a maximum of 15 double-image frames per second, with time intervals between two images of a frame as low as 1 μs. The timings of the laser firing and image capture are controlled by a synchronizer unit. Ensemble cross correlation scheme (Meinhart et al. 2000) together with background conditioning was used for deriving the flow field from an average 50 double-frame images. Flow through the microchannels is maintained and controlled by a precision syringe pump (KD Scientific, MA).

3 Results and discussion

A solution of sodium hydroxide, pH = 12.5 and pH indicator (phenolphthalein), prepared in 60% isopropanol, water balance (similar kinematic viscosity) are pumped into the microchannel using the infusion pump at identical flow rates. Since all physical properties remain constant, the flow rate can be changed to achieve various Re numbers. When the two liquids mix, the transparent solutions turn into pink/purple color, showing the extent of diffusion (Fig. 5). Figure 6 shows the development of mixing at 12 mm from the inlet of the T-mixer and Σ-micromixer. The Σ-micromixer clearly shows better ability to mix the flow passively and thoroughly. Since fluids in the Σ-mixer travel curved paths, a corrected length, L, is used in data representation to account for the added length in the serpentine channel.

Based on the earlier analysis, if velocities at the diffusion interfaces of the two fluids are increased, the diffusive flux would increase. From Eq. 6, it can be seen that the diffusion increases with increase in the interface velocity. But because the diffusive interface shifts away from the centerline along the channel, the proposed sidewalls alter the flow passively, such that diffusion occurs at a relatively larger interfacial velocity on diffusion fronts.

In order to quantify the diffusion process, color images at select cross sections are converted into gray-scale images, following Ref (Lee et al. 2006). The images are saved for image processing using MATLAB® image processing toolbox. In the four color schemes given in Fig. 5b, the first

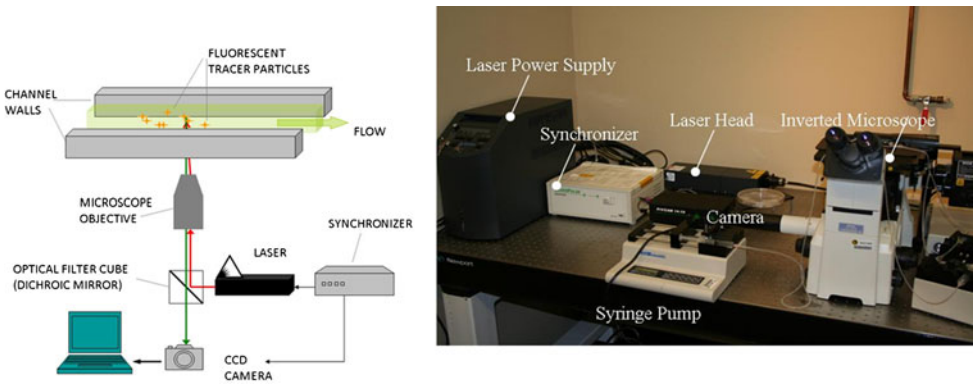

Fig. 4 Micro-particle image velocimetry setup

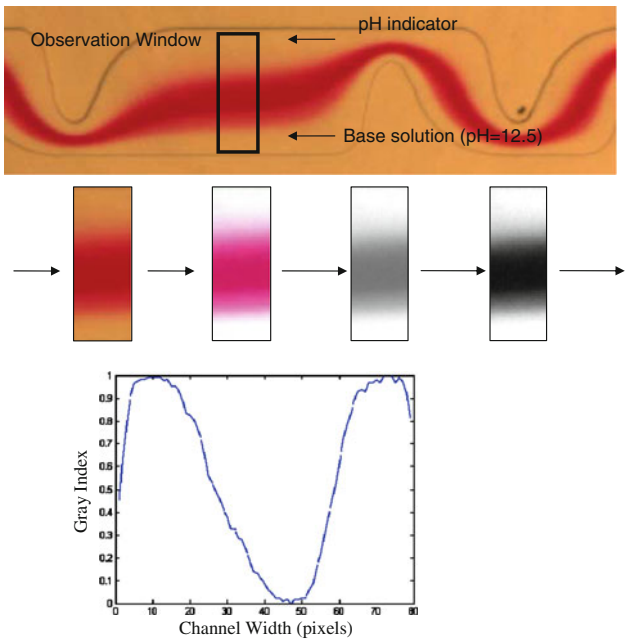

Fig. 5 Evaluation of mixing performance using color changes as a result of mixing of a pH indicator (phenolphthalein) and a base solution (sodium hydroxide, pH = 12.5). Image processing includes color enhancement, conversion to grayscale, contrast improvement and evaluation of gray index across the channel width. Ideal case is that all pixels attain gray index, $I = 0$. Mixing percentage is calculated based on measuring the deviation of the cross section pixels' *gray* index from the ideal value

image represents the cropped image noting the width and the length pixels; the second image represents the enhanced color; the third image is the image read into the toolbox and converted to grayscale; the fourth image represents the image with enhanced contrast. After rescaling the contrast from 0 to 1, the grayscale of a middle column across the width of the channel is shown in Fig. 5c. The deviation of gray intensity around the darkest gray pixel (completely mixed region in the middle of the channel) is calculated for the pixels of the selected cross section using the following equation (Stroock et al. 2002):

$$\sigma = \left[\frac{1}{n}\sum_{i=1}^{n}(I_{\min} - I_i)^2\right]^{1/2} \tag{8}$$

where n is the number of the cross section pixels, I_i is gray intensity of pixel i of the selected cross section and $I_{\min}$ is the minimum gray intensity. When there is no mixing, the standard deviation, $\sigma = 1$, and ideally at full mixing it will reach 0 as all pixels attain uniform gray intensity. Using the definition of standard deviation in Eq. 8, mixing percentage is defined as

$$M(\%) = (1 - \sigma) \times 100 \tag{9}$$

Pixels with gray intensity of $I = 0$ show fully mixed regions whereas bright pixels, $I = 1$, are non-mixed portions of the flow (Fig. 7).

Mixing performance can be characterized as a function of flowrate (or Re number) and mixer length as shown in Figs. 8 and 9, respectively. Both micromixers show similar dependence on flowrate and downstream length. As the Reynolds number increases, the residence time in the mixing channel becomes very short and the mixing is not very efficient. This is a typical behavior of all diffusion-based mixers including the presently analyzed T-junction, and the Σ-micromixer. However, the overall performance of the Σ mixer with periodic flow variation is better than the T-mixer since fluids in a T-mixer attain a non-varying parabolic velocity profile at set conditions. While diminished mixing for increasing Reynolds number at a given mixer length is observed, results show that for a constant Reynolds number, mixing progresses downstream of the channels. Major increase in the mixing percentage for both channels occurs within the first few millimeters from the entrance. However, Σ-micromixer continues to improve mixing downstream the channel.

Mixing decreases with an increase in the flow rate observing a power law. The slope of $M\%$ versus Re on a logarithmic scale is constant and negative as also seen by (Ismagilov et al. 2000). It was found that at steady state, the

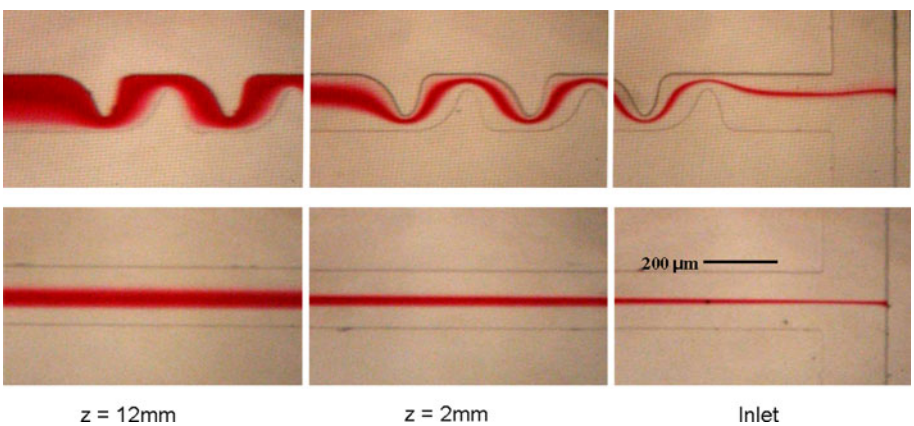

Fig. 6 Flow visualization in a T-junction and Σ-mixer and at Re = 0.55 (600 µl/h). The three views show mixing from in a 1-mm segment at inlet, 2 mm from inlet ($L = 2.6$ mm) and 12 mm from inlet ($L = 15.5$ mm)

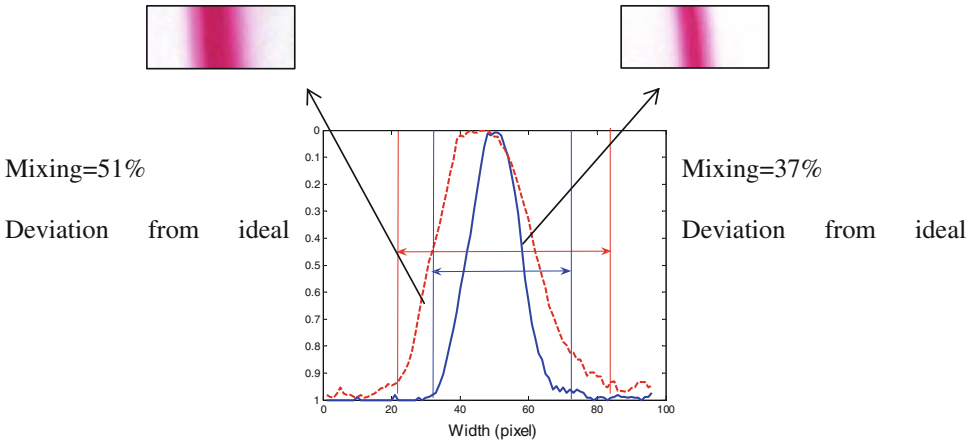

Fig. 7 Correlation between color (gray index) and the extent of mixing. Ideal mixing (completed chemical reaction) corresponds to gray index ($I = 0$) and that deviation between gray indices (σ) across the width of the channel be zero

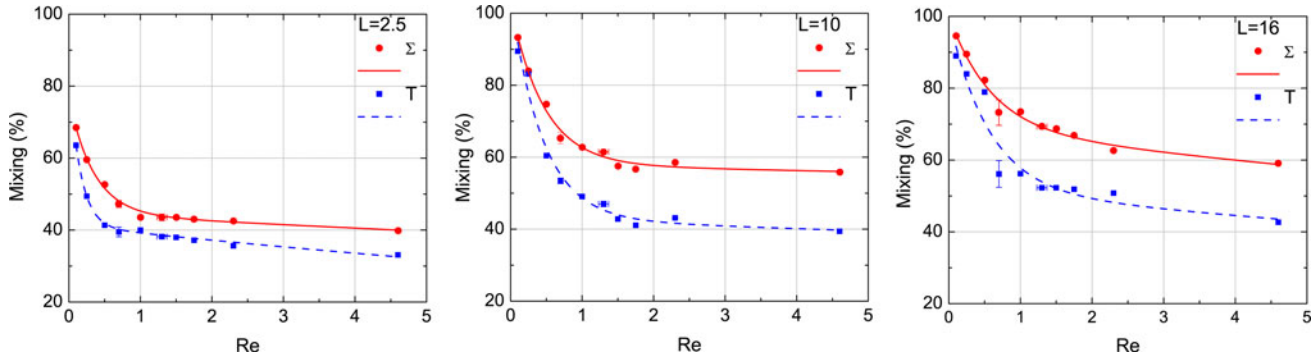

Fig. 8 Dependence of mixing on flow rate (Re) at a given corrected mixer lengths. Overall enhancement of mixing performance is observed for the Σ channel with variable flow profile

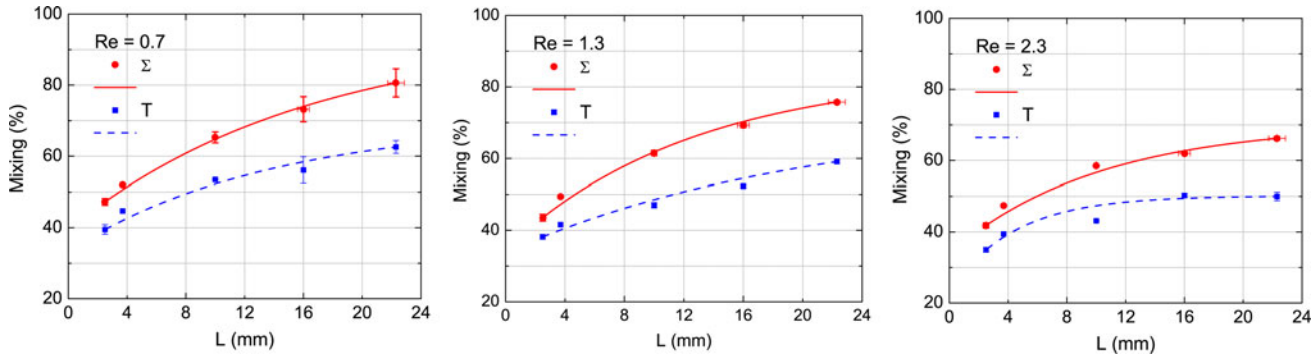

Fig. 9 Dependence of mixing on mixer lengths (corrected length is used to account for the curved path of the serpentine Σ mixer). Overall enhancement of mixing performance is observed for the Σ channel with variable flow profile

decrease in the width of the reaction–diffusion zone at the interface of miscible streams scales to one-half power of flow rate at the core of the flow and to one-third power adjacent to the walls of the channel. Similar scaling factors have been found for increase in the diffusion band with increasing streamwise length. The current experimental results display this power law as given in Fig. 10, which indicates a negative slope of mixing efficiency with Reynolds number (−0.25 and −0.15 for T-mixer and Σ-mixer, respectively) and a positive slope for increasing mixer length (0.19 and 0.25 for T-mixer and Σ-mixer, respectively). The constant slopes show that both mixers operate in a diffusion-dominated regime. The experiments were extended up to Re = 4.6; however, at higher Re, the regime would change to an inertia dominated one and the performance of the Σ mixer might improve.

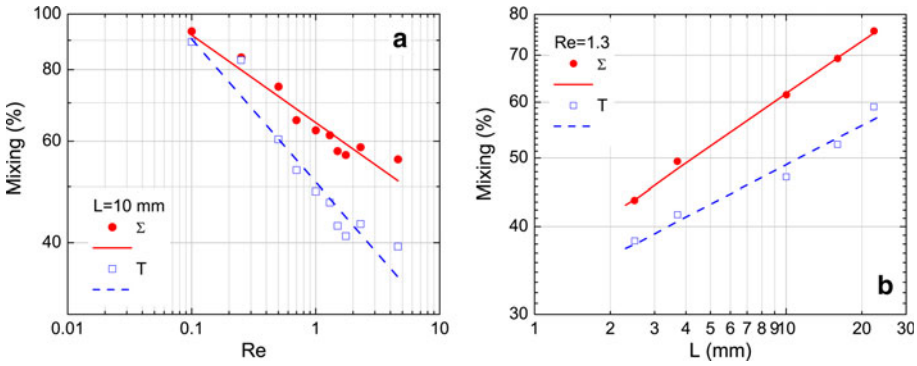

Fig. 10 Logarithmic dependence of diffusive mixing on **a** flowrate [slope $\Sigma = -0.15$, slope $T = -0.25$] and **b** mixer length [slope $\Sigma = 0.25$, slope $T = 0.19$]

In order to understand the physics behind the diffusion process and to validate the hypothesis that the velocity profile variation contributes to mixing, micro-PIV studies are undertaken next. The tracer particles used for μPIV are dispersed homogenously in water and fed into the devices using an infusion pump. The same mixture with identical tracer particle concentration is used for all the test cases. The size of the tracer particles (1 μm on average) is much smaller than typical dimensions of the flow device, which ensures that the particles would follow the flow reasonably well. The response time of a particle subjected to a step change in local fluid velocity can be used as a measure of how well the particle is able to follow the flow. First-order response to a constant flow acceleration (assuming Stokes flow for the particle drag), the response time is given by $\tau = \frac{d^2\rho_p}{18\mu}$ where d and ρ_p are the diameter and density of seeding particles and μ is the dynamic viscosity of the fluid. For the current experiments that involve polystyrene particles in water: (d: 1 μm, ρ_p: 1.05 g/cm^3), the response time of seeding particles is on the order of 1.1×10^{-6} s. The typical time interval used in the current experiment for PIV imaging is on the order of a few hundred microseconds. Comparing the response time of particles with the time interval, the particles will follow the flow well. The border of the channels, as observed through the microscope, consists of a line with two edges; each representing the intersection of the sidewall with the top and the bottom wall. The objective lens is adjusted carefully to pinpoint the upper and lower walls and calibrate the microscope focus with the actual microchannel depth.

The camera records digital images of 512 × 480 pixels of an area of 600 × 400 μm resulting in 1 μm^2/pixel. If the diameter of a particle image is resolved over 3–4 pixels, then the uncertainty in determining particle displacement can be found to within one tenth of the particle-image diameter (Santiago et al. 1998). Since seeding particles occupy approximately 3 pixels (projected area of a particle is 3.14 μm^2), the displacement of each particle is found to 0.1 μm accurate. Using an average of 200-μs time intervals in the experiments, the measured velocity would have an uncertainty of 0.5 mm/s. The average velocity for a flow rate of 1,000 μl/h in this work is ∼13 mm/s, leading to an error in velocity measurement of ∼4%. In μPIV, all the particles in the flow field are illuminated (volume illumination) due to limited optical access. In most cases, information on the depthwise coordinate is lost and a two-dimensional average field is obtained. In this work, a 4× magnification lens with numerical aperture 0.1 was used. This provided a depth of focus of 55 μm (channel height is 100 μm), therefore, does not provide resolution of the depth coordinate of the flow. The focus was at the center plane which provided a two-dimensional average of the flow, but a wider field allowed a larger portion to be visualized. The two-dimensional representation of flow at a certain depth serves our purpose of demonstrating the periodic variation of laminar flow and its correspondence to enhancing diffusive mixing based on the concept of increasing interfacial velocity.

PIV visualization images show the passive and periodic variation of the laminar flow profile in the mixing channel. Figure 11 shows the PIV flow visualization in the channel. The variation of velocity profile is achieved passively by the appropriate design of the sidewalls. It is seen that a clear variation of the flow profile (shifting of the maximum) is observed when compared to the non-varying parabolic profile in a straight channel. The depth of the channels is comparable to the width of the channel; therefore, flow is three dimensional. However, μPIV images provided here are 2D representations of the flow because the depth of the channel cannot be easily resolved due to volume illumination (Olsen and Adrian 2000) when compared to conventional PIV where it is possible to image single slices of flow by generating thin 2D light sheets. In addition to reducing signal to noise, out of focus tracking particles contribute to the average-based cross correlation algorithms. Several techniques have been proposed in order resolve issues arising from volume illumination in μPIV flow measurements including particle visibility thresholds

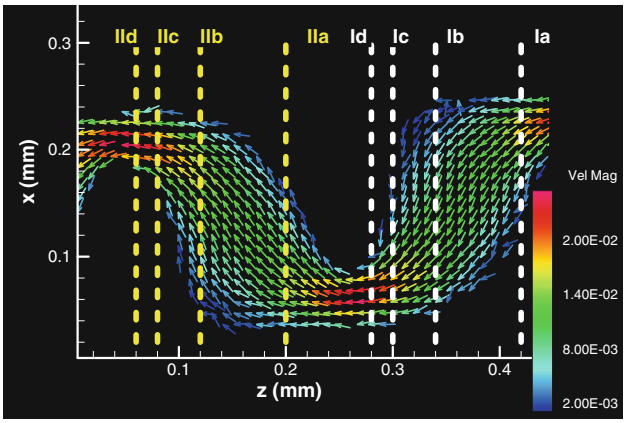

Fig. 11 Vector plot of velocity magnitude (mm/s) in one pass of the mixer channel. Sections group I and II are half the periodic length (λ) apart

(Olsen and Adrian 2000) and light-intensity filtering (Bourdon et al. 2004). The two-dimensional representation is sufficient for our analysis and discussion since velocity profiles at locations along the streamwise direction are compared.

Sections I and II in Fig. 11 are taken at comparable locations which are a half wave-length apart. Velocity profiles are shown for these sections in Figs. 12 and 13 for Reynolds numbers of 0.37 and 3.0, respectively. Velocity is normalized by the respective average flow velocity and plotted against the normalized channel width. The velocity profiles at comparable sections of I and II are seen to be reversed; i.e., layers of fluid close to one wall which move at higher speeds in one section decelerate in the following section where layers close to the opposite wall accelerate. The shift in the velocity peak across the transverse direction causes diffusion to occur faster than in the straight channel. Mainly, at low Re number flows, diffusion is higher due to larger residence time of species in the mixer channel and for higher Reynolds numbers, the residence time is shorter and the mixing is not very efficient. However, by comparing the velocity profiles in Figs. 12 and 13, the normalized velocity peaks are nearly two times larger for Re = 0.37 than for Re = 3.0 at every cross section where measurements were made. In other words, flow variation is found to be more pronounced and effective for enhancing the passive diffusive mixing in the low Re number regime which is the working range of most microfluidic devices.

Figure 14 shows the periodic variation of the locus of the velocity peaks across the width downstream of the channel. Despite a slight mismatch, the extent of deviation for both Reynolds numbers is of the same order; about $w^* = 0.25$ on each side of the centerline with a similar pattern. For both Σ-mixer and T-mixer, the mixing rapidly deteriorates at high Reynolds numbers because species are in contact for extremely short times where diffusion is significantly reduced.

4 Conclusions

It was found that (1) diffusive mass flux between streams of fluid flowing in a laminar regime increases as the velocity of the interface between the streams of liquid increases and (2) in a micromixing channel, the diffusion interfaces progress in the transverse direction as the flow moves downstream. Based on these two findings, it is shown that significant improvement in mixing can be achieved by passively shifting the maximum of the velocity profile from the centerline to coincide with the transversely

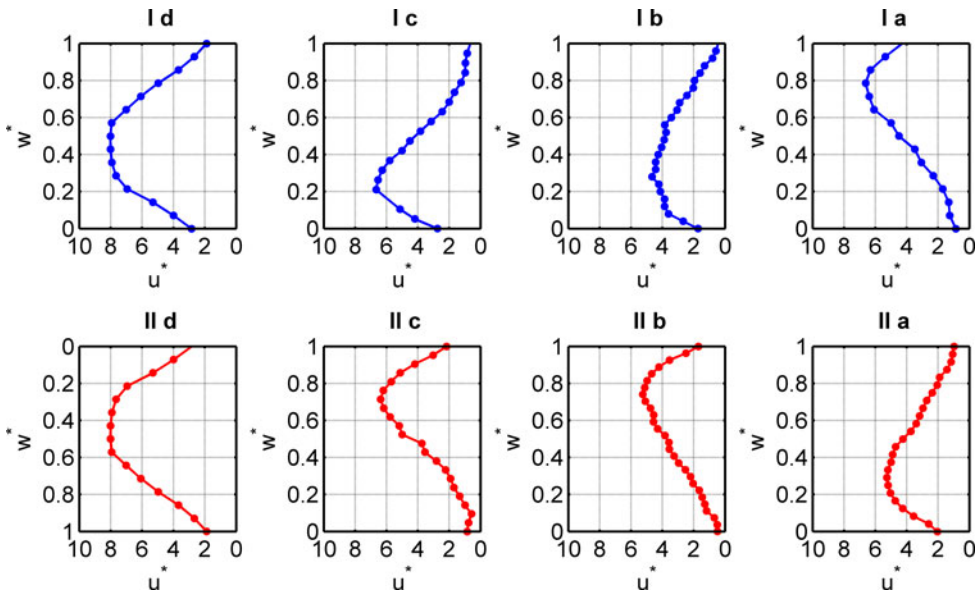

Fig. 12 Velocity profiles at sections I and II for Re = 0.37. Local velocity is normalized by the average velocity. Cross-section references are as given in Fig. 9

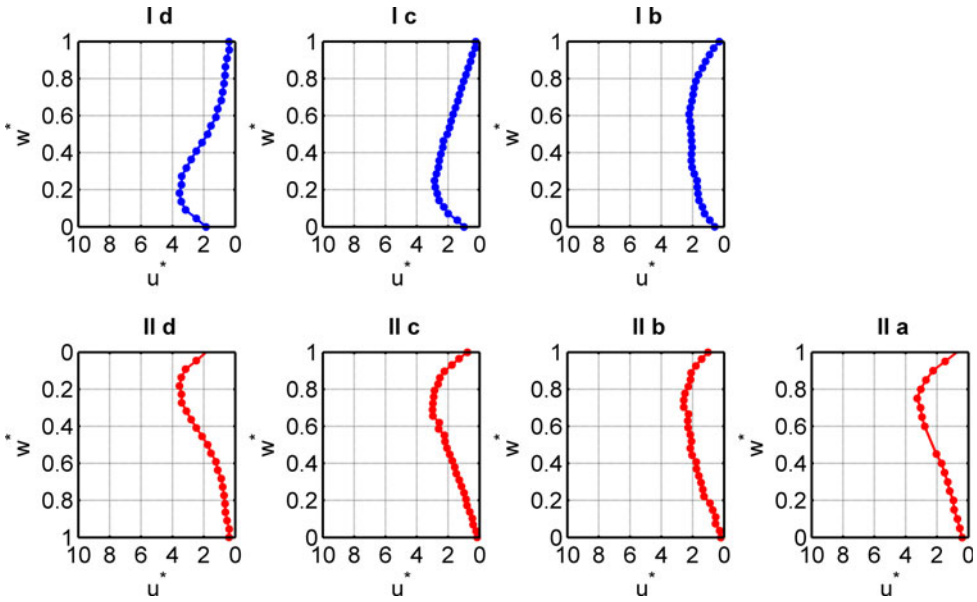

Fig. 13 Velocity profiles at sections I and II for Re = 3. Local velocity is normalized by the average velocity. Cross-section references are as given in Fig. 11

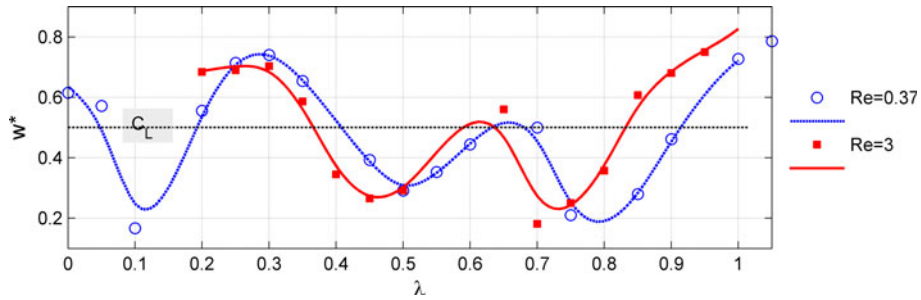

Fig. 14 Shift of the velocity peak across the channel width found by particle image velocimetry flow visualization

moving interfaces as often as possible during the residence time of the fluids in the mixer channel.

A simple passive micromixer, called the Σ-micromixer, has been fabricated and tested. Its functionality was verified experimentally by quantifying color variations, resulting from mixing of phenolphthalein (pH indicator) and sodium hydroxide. Experimental results from mixing and flow visualization sections show the periodic variation of the velocity profile such that its maximum shifts across the transverse direction in a periodic manner. As a result, diffusion across layers occurs with a relatively higher velocity, hence larger mass flux and diffusive mixing. In contrast, in a straight channel, when diffusion fronts move away from the centerline, they overlap on slow moving layers of fluid resulting in poor mass flux and less progress in mixing downstream. Finally, since the nature of mixing is diffusion-based and a power law dependence on flow rate and mixer length has been established, the significance and effectiveness of flow profile variation for augmented diffusion is proven.

The Σ-micromixer can be adopted for a wide-range of microfluidic applications in the low Reynolds number flows. The planar design facilitates the fabrication and integration of the micromixer which is advantageous for the disposable polymer-based biochemical assay chips. The micromixer has no recirculation zones. The variability of cross-section velocity in a laminar flow and maintaining highest possible surface area between miscible streams are found to be essential factors for enhanced passive diffusion-dominated micromixing.

Acknowledgments This work was supported by National Science Foundation (ECS 0348603 and ECCS 0901503) and Korea Science and Engineering Foundation (WCU program, R32-2008-000-10124-0).

References

Bird RB, Stewart WE, Lightfoot EN (2007) Transpot phenomena. Wiley, New York

Bourdon CJ, Olsen MG, Gorby AD (2004) Power-filter technique for modifying depth of correlation in microPIV experiments. Exp Fluids 37:263–271

Deshmukh AA, Liepmann D, Pisano AP (2001) Continuous micromixer with pulsatile micropumps Solid-State Sensor and Actuator Workshop. Hilton Head Island

Hardt S, Drese KS, Hessel V, Schonfeld F (2005) Passive micromixers for applications in the microreactor and uTAS fields. Microfluidics and Nanofluidics pp 108–118

Hong CC, Choi JW, Ahn CH (2004) A novel in-plane passive microfluidic mixer with modified Tesla structures. Lab Chip 4:109–113

Ismagilov RF, Stroock AD, Kenis PJA, Whitesides G, Stone HA (2000) Experimental and theoretical scaling laws for transverse diffusive broadening in two-phase laminar flows in microchannels. Appl Phys Lett 76:2376–2378

Jen CP, Wu CY, Lin YC, Wu CY (2003) Design and simulation of the micromixer with chaotic advection in twisted microchannels. Lab Chip 3:77–81

Kamholz AE, Yager P (2001) Theoretical analysis of molecular diffusion in pressure-driven laminar flow in microfluidic channels. Biophys J 80:155–160

Lee SW, Kim DS, Lee SS, Kwon TH (2006) A split and recombination micromixer fabricated in a PDMS three-dimensional structure. J Micromech Microeng 16:1067–1072

Liu RH, Stremler MA, Sharp KV, Olsen MG, Santiago JG, Adrian RJ, Aref H, Beebe DJ (2000) Passive mixing in a three-dimensional serpentine microchannel. J Microelectromech Syst 9:190–197

Liu RH, Yang J, Pindera MZ, Athavale M, Grodzinski P (2002) Bubble-induced acoustic micromixing. Lab Chip 2:151–157

Liu Y, Olsen MG, Fox RO (2009) Turbulence in a microscale planar confined impinging-jets reactor. Lab Chip 9:1110–1118

Meinhart CD, Wereley ST, Santiago JG (2000) A PIV algorithm for estimating time-averaged velocity fields. J Fluids Eng 122: 285–289

Melin J, Giménez G, Roxhed N, Wvd Wijngaart, Stemme G (2004) A fast passive and planar liquid sample micromixer. Lab Chip 4:214–219

Nguyen N-T, Wu Z (2005) Micromixers-a review. J Micromech Micoreng 15:R1

Nichols KP, Ferullo JR, Baeumner AJ (2005) Recirculating, passive micromixer with a novel sawtooth structure. Lab Chip 6:242–246

Oddy MH, Santiago JG, Mikkelsen JC (2001) Electrokinetic instability micromixing. Anal Chem 73:5822–5832

Olsen MG, Adrian RJ (2000) Out-of-focus effects on particle image visibility and correlation in microscopic particle image velocimetry. Exp Fluids 29:S166–S174

Santiago JG, Wereley ST, Meinhart CD, Beebe DJ, Adrian RJ (1998) A particle image velocimetry system for microfluidics. Exp Fluids 25:316–319

Schonfeld F, Hessel V, Hofmann C (2004) An optimised split-and-recombine micro-mixer with uniform chaotic mixing. Lab Chip 4:65–69

Stroock AD, Dertinger SKW, Ajdari A, Mezic I, Stone HA, Whitesides GM (2002) Chaotic mixer for microchannels. Science 295:647–651

Tofteberg T, Skolimowski M, Andreassen E, Geschke O (2009) A novel passive micromixer: lamination in a planar channel system. Microfluid Nanofluidics 8:209–215

Tsai J-H, Lin L (2002) A thermal-bubble-actuated micronozzle-diffuser pump. J Microelectromech Syst 11:665–671